

# **SANDIA REPORT**

SAND2015-8808

Unlimited Release

Printed Sept. 2015

## **Sensitivity Analysis of OECD Benchmark Tests in BISON**

Laura P. Swiler, Kyle A. Gamble, Rodney C. Schmidt, Richard L. Williamson

Prepared by  
Sandia National Laboratories  
Albuquerque, New Mexico 87185 and Livermore, California 94550

Sandia National Laboratories is a multi-program laboratory managed and operated by Sandia Corporation, a wholly owned subsidiary of Lockheed Martin Corporation, for the U.S. Department of Energy's National Nuclear Security Administration under contract DE-AC04-94AL85000.

Approved for public release; further dissemination unlimited.



**Sandia National Laboratories**



Issued by Sandia National Laboratories, operated for the United States Department of Energy by Sandia Corporation.

**NOTICE:** This report was prepared as an account of work sponsored by an agency of the United States Government. Neither the United States Government, nor any agency thereof, nor any of their employees, nor any of their contractors, subcontractors, or their employees, make any warranty, express or implied, or assume any legal liability or responsibility for the accuracy, completeness, or usefulness of any information, apparatus, product, or process disclosed, or represent that its use would not infringe privately owned rights. Reference herein to any specific commercial product, process, or service by trade name, trademark, manufacturer, or otherwise, does not necessarily constitute or imply its endorsement, recommendation, or favoring by the United States Government, any agency thereof, or any of their contractors or subcontractors. The views and opinions expressed herein do not necessarily state or reflect those of the United States Government, any agency thereof, or any of their contractors.

Printed in the United States of America. This report has been reproduced directly from the best available copy.

Available to DOE and DOE contractors from

U.S. Department of Energy  
Office of Scientific and Technical Information  
P.O. Box 62  
Oak Ridge, TN 37831

Telephone: (865) 576-8401  
Facsimile: (865) 576-5728  
E-Mail: [reports@adonis.osti.gov](mailto:reports@adonis.osti.gov)  
Online ordering: <http://www.osti.gov/bridge>

Available to the public from

U.S. Department of Commerce  
National Technical Information Service  
5285 Port Royal Rd.  
Springfield, VA 22161

Telephone: (800) 553-6847  
Facsimile: (703) 605-6900  
E-Mail: [orders@ntis.fedworld.gov](mailto:orders@ntis.fedworld.gov)  
Online order: <http://www.ntis.gov/help/ordermethods.asp?loc=7-4-0#online>



## **Sensitivity Analysis of OECD Benchmark Tests in BISON**

Laura Swiler  
Optimization and Uncertainty Quant.  
Sandia National Laboratories  
P.O. Box 5800  
Albuquerque, NM 87185-1318  
lpswile@sandia.gov

Rodney Schmidt  
Severe Accident Analysis  
Sandia National Laboratories  
P.O. Box 5800  
Albuquerque, NM 87185-0748  
rschmi@sandia.gov

Kyle Gamble  
Fuel Modeling and Simulation  
Idaho National Laboratory  
2525 Fremont Avenue  
Idaho Falls, ID 83415  
kyle.gamble@inl.gov

Richard Williamson  
Fuel Modeling and Simulation  
Idaho National Laboratory  
2525 Fremont Avenue  
Idaho Falls, ID 83415  
richard.williamson@inl.gov

### **Abstract**

This report summarizes a NEAMS (Nuclear Energy Advanced Modeling and Simulation) project focused on sensitivity analysis of a fuels performance benchmark problem. The benchmark problem was defined by the Uncertainty Analysis in Modeling working group of the Nuclear Science Committee, part of the Nuclear Energy Agency of the Organization for Economic Cooperation and Development (OECD). The benchmark problem involved steady-state behavior of a fuel pin in a Pressurized Water Reactor (PWR). The problem was created in the BISON Fuels Performance code. Dakota was used to generate and analyze 300 samples of 17 input parameters defining core boundary conditions, manufacturing tolerances, and fuel properties. There were 24 responses of interest, including fuel centerline temperatures at a variety of locations and burnup levels, fission gas released, axial elongation of the fuel pin, etc. Pearson and Spearman correlation coefficients and Sobol' variance-based indices were used to perform the sensitivity analysis. This report summarizes the process and presents results from this study.

## **ACKNOWLEDGMENTS**

This work was funded by the Nuclear Energy Advanced Modeling and Simulation (NEAMS) Program under the Advanced Modeling and Simulation Office (AMSO) in the Nuclear Energy Office in the U.S. Department of Energy. The authors specifically acknowledge the Program Manager of the Integrated Product Line, Dr. David Pointer (ORNL), and Dr. Marius Stan, National Technical Director of NEAMS, for their support of this work. Finally, we thank the Dakota, BISON, and MOOSE development teams.

# CONTENTS

1. Introduction.....	7
1.1 BISON.....	7
1.2 Case 2a BISON model.....	7
1.3 Dakota.....	8
2. SENSITIVITY ANALYSIS and uncertainty quantification .....	11
2.1. Latin Hypercube Sampling .....	11
2.2 Sensitivity Analysis: Correlation coefficients .....	12
2.3 Sensitivity Analysis: Variance-based Decomposition.....	13
3. OECD Case 2a Results .....	15
4. Conclusions.....	23
5. References.....	24
APPENDIX A.....	26
APPENDIX B .....	27
Distribution .....	29



# 1. INTRODUCTION

This report summarizes a NEAMS (Nuclear Energy Advanced Modeling and Simulation) project focused on sensitivity analysis of a fuels performance benchmark problem. The benchmark problem was defined by the Uncertainty Analysis in Modeling working group of the Nuclear Science Committee, part of the Nuclear Energy Agency of the Organization for Economic Cooperation and Development (OECD) in the report “Benchmark for Uncertainty Analysis in Modelling (UAM) for Design, Operation, and Safety Analysis of LWRs”, hereafter referred to as the “Benchmark report” and given in Reference [1]. The benchmark problem involved steady-state behavior of a fuel pin in a Pressurized Water Reactor (PWR). The problem analyzed in this report is Case 2a, defined in Chapter 2 of the Benchmark report. Chapter 2, titled “Definition of Exercise II-1: Fuel Modelling,” has detailed descriptions of the test problems, along with boundary conditions, manufacturing tolerances, and fuel properties for various cases.

As stated by the Benchmark report, the goal of the UAM committee is “focused on identifying and propagating input uncertainties through fuel performance codes.”[1, Chapter 2] Specifically, the committee wanted to compare “the evaluation of uncertainties associated with modelling and prediction of the fuel behavior”[1, Chapter 2] across a variety of codes and using several approaches. For the purposes of this study, we used the BISON code to model the Case 2a problem, and the Dakota code to perform sensitivity analysis (SA) and uncertainty quantification (UQ).

The outline of this report is as follows: the remainder of this section describes BISON and Dakota in more detail. Section 2 outlines the sensitivity analysis and uncertainty quantification methods used. Section 3 provides results, and Section 4 presents the conclusions.

## 1.1 BISON

BISON is an implicit, parallel, fully-coupled nuclear fuel performance code under development at the Idaho National Laboratory (INL) [2]. BISON is built on the MOOSE computational framework [3] which allows for rapid development of codes involving the solution of partial differential equations using the finite element method. Nuclear fuel operates in an environment with complex multiphysics phenomena, occurring over distances ranging from inter-atomic spacing to meters, and time scales ranging from microseconds to years. This multiphysics behavior is often tightly coupled and many important aspects are inherently multidimensional.

BISON is able to simulate tightly coupled multiphysics and multiscale fuel behavior, for 1D, 2D, and 3D geometries. BISON code validation and assessment is presented in [4]. In BISON, there are several physical processes that may affect the thermal behavior of a fuel rod during normal operation. The Bison Theory Manual [5] provides a description of the models currently coded in BISON.

## 1.2 Case 2a BISON model

The BISON model created for the Case 2a study used the smeared-pellet mesh capability in BISON. A smeared mesh was used to make coupling to Dakota easier for sensitivity and uncertainty quantification. BISON has an internal mesh generation tool that only generates smeared fuel rods for LWR fuel performance analyses. If a discrete mesh is desired the external

Cubit mesh script must be used. By utilizing the internal mesh script it provides hooks to uncertain dimensional parameters such as the fuel pellet outer diameter, cladding thickness, and gap thickness that can be easily varied by Dakota. Note that the smeared mesh means that the individual pellets are not modeled and the entire fuel stack is essentially treated as one right cylinder (once revolved about the axisymmetric axis). The evolution of the gap between the pellet and cladding is modeled during the simulation prior to and after contact. The heat transfer coefficient of the gap is modeled using a modified version of the model proposed by Ross and Stoute (AECL 1962, Ref. 17). In short the pellet-to-cladding mechanical and thermal interaction is accurately modeled even when using a smeared mesh.

The fuel rod was modeled as a 2-D axisymmetric R-Z simulation. The BISON model had 4290 QUAD8 elements resulting in approximately 324000 total degrees of freedom (including both nonlinear variables and the auxiliary system (e.g., stresses, contact pressure)), and took approximately 4.5 hours to run on 12 cores of INL's Fission High Performance Computing machine.

Eleven radial elements were used in the fuel to properly capture the radial power profile that captures the plutonium buildup in the rim region of the fuel pellet during irradiation. Three radial elements were used through the cladding thickness to ensure proper determination of the stress within the clad. All parameters of interest required for postprocessing, sensitivity analyses, and uncertainty quantification are output at each time step as a postprocessor into a CSV file.

### **1.3 Dakota**

To perform the sensitivity and uncertainty analysis, we interfaced a toolkit called Dakota to the BISON fuel performance code on Fission at Idaho National Laboratory. Dakota allows a user to design computer experiments, run parameter studies, perform uncertainty quantification, and calibrate parameters governing their simulation model. A primary goal for Dakota is to provide scientists and engineers with a systematic and rapid means to obtain improved or optimal designs or understand sensitivity or uncertainty using simulation-based models. These capabilities generally lead to improved designs and better understanding of system performance [6].

One of the primary advantages that Dakota has to offer is access to a broad range of iterative capabilities through a single, relatively simple interface between Dakota and a simulator. In this context, we interfaced Dakota to BISON. To perform different types of analyses, it is only necessary to change a few commands in the Dakota input and start a new analysis. The need to learn a completely different style of command syntax and the need to construct a new interface each time you want to use a new algorithm are eliminated.

The coupling between Dakota and BISON is shown in Figure 1. The Dakota executable is controlled by a text input file which specifies the parameters, the responses, and the analysis method to be used (in this case, it was a sampling study). Dakota writes a separate parameters file for each evaluation of the BISON simulation code. This parameters file is used by a script that "drives" the analysis (the analysis\_driver script). The purpose of the script is to take the parameters file, use a text processing capability to substitute the Dakota-sampled parameter values into the BISON input deck, run BISON (e.g. submit the job to the queue), then extract the



results and return the appropriate response values to Dakota. Thus, the `analysis_driver` script does some pre-processing, runs the simulation, and then does some postprocessing. When the results are returned to Dakota, Dakota then starts another function evaluation and creates another parameters file. At the end of all of the samples, Dakota calculates the first four moments (mean, variance, skewness, kurtosis) of the responses, and also calculates correlation coefficients. Dakota summarizes the runs in a tabular output file that can be imported to Excel or another tool.

Note that the OECD Benchmark problem required centerline temperatures at specified burnup values. The selected temperature measurements were obtained by selecting the node at the pellet centerline at the particular axial location of interest. In BISON, it is not possible to force a time step at a particular burnup. To populate the OECD spreadsheet for case 2a, we developed a postprocessing code to find the 2 lines in the BISON csv output file bracketing a specified burnup value and perform a linear interpolation to obtain the results at the desired burnup value.

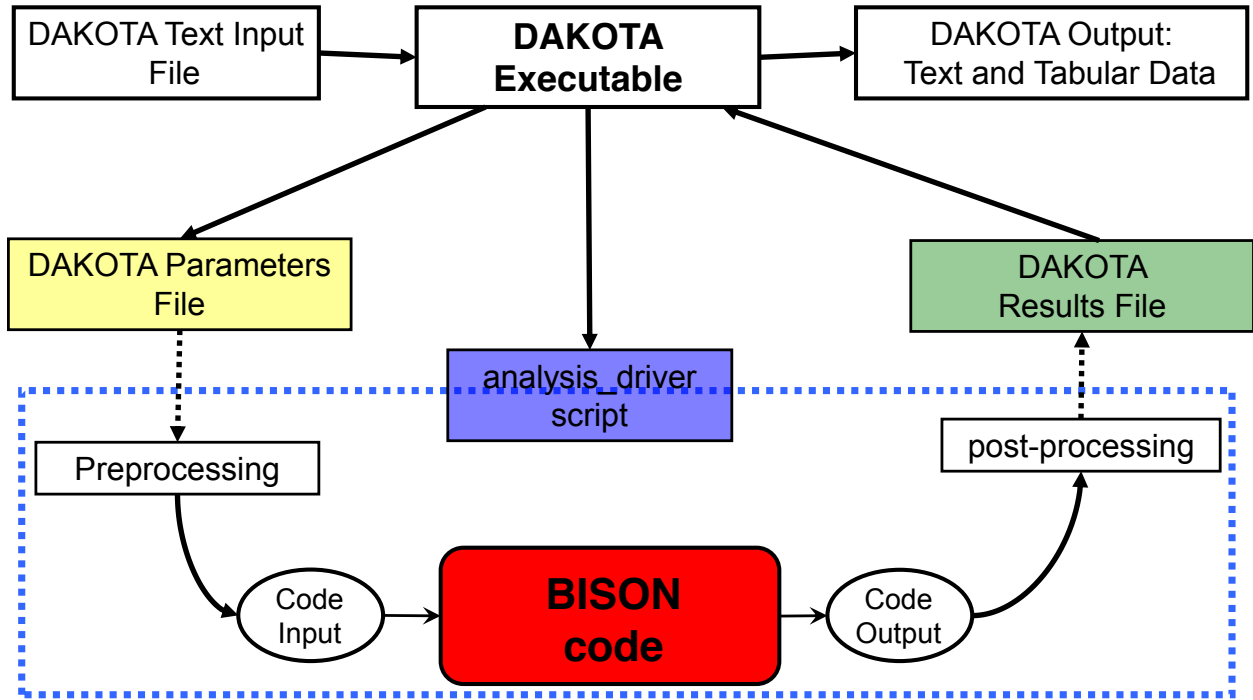


Figure 1: Information Flow between Dakota and BISON for the Sampling Studies



## 2. SENSITIVITY ANALYSIS AND UNCERTAINTY QUANTIFICATION

The OECD Benchmark team asked the analysis groups to produce two types of results for the benchmark cases: (1) a ranking of the input parameters using sensitivity analysis and (2) the quantification of the uncertainty on the output responses. For the sensitivity analysis task in (1), the OECD team recommended that a Pearson or Spearman Rank correlation coefficient be used. We used a Spearman Rank correlation coefficient (SRCC). We also examined the use of Sobol' main effects indices. For the uncertainty quantification task (2), the OECD wanted estimates of the mean and the standard deviation of the output responses.

Dakota has a variety of sensitivity analysis methods, including design of computer experiments, orthogonal arrays, the Morris-one-at-a-time method, and variance-based decomposition. Dakota also has a variety of uncertainty quantification algorithms, including sampling methods, reliability methods, polynomial chaos expansions, interval analysis, etc. For this project, we chose to use Latin Hypercube sampling (LHS), in part because we could use the same LHS study for both the sensitivity analysis and the uncertainty quantification, and in part because LHS produces the SA/UQ metrics the OECD team requested. In the future, we plan to examine other methods.

The following paragraphs provide a more detailed description of LHS and the sensitivity methods used for the interested reader.

### 2.1. Latin Hypercube Sampling

The most common method of incorporating uncertainty into simulations is to assume particular distributions on the uncertain input values, then randomly sample from those distributions, run the model with the sampled values, and do this repeatedly to build up a distribution of the output values. This is classical statistical Monte Carlo (MC) propagation of uncertainty. The output values can be analyzed to determine characteristics of the response (e.g. what are the maximum and minimum response values, what is the mean and the variance of the response, how skewed is the response distribution, etc). The main advantage of Monte Carlo sampling is that the accuracy and computational burden is essentially independent of the number of uncertain parameters. A disadvantage of MC sampling is the cost. To get accurate estimates for the statistics obtained directly from the random samples, one must have a large number of samples. The accuracy of the mean estimate obtained from a set of random samples displays  $1/\sqrt{N}$  convergence, meaning that on average one needs to quadruple the number of sample points to halve the error.

A good alternative to pure random sampling is **Latin Hypercube Sampling (LHS)** [7,8]. LHS is a stratified random sampling method where the distribution is divided into strata or bins. Each stratum is chosen to be equally probable, so that the strata are of equal length for uniform distributions but of unequal length for normal distributions. For example, the strata near the center of normal distributions are shorter than the strata near the tails. If one wants to create a total sample of size  $N$  using LHS, an individual sample value is chosen from each of the  $N$  equally probable strata for each input variable. This stratification approach serves to force a better sampling across the entirety of each distribution and eliminates some of the clustering of sample points often seen in pure random sampling. LHS is more efficient than pure Monte Carlo in the sense that it requires fewer samples to achieve the same accuracy in statistics

(standard error of the computed mean, for example). LHS gives an estimator for a function mean that has lower variance than MC for any function having finite second moment [9, 10]. Further, the convergence behavior of LHS improves if the function is additively separable, meaning it can be decomposed into additive functions of the individual input parameters.

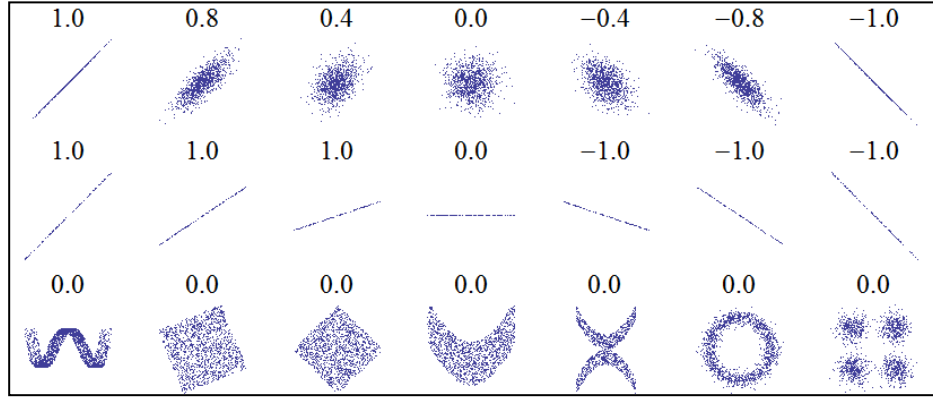
## 2.2 Sensitivity Analysis: Correlation coefficients

The purpose of sensitivity analysis is to identify the most significant factors or variables affecting the uncertainty of the model predictions. Here we summarize two approaches to sensitivity analysis: correlation analysis and variance-based decomposition. These are described below. For greater detail, the reader is encouraged to refer to one of the books published by a group at the European Research Commission on sensitivity analysis, such as [11, 12].

Correlation refers to a statistical relationship between two random variables or two sets of data. The main focus of correlation analysis of computer experiments is the correlation between inputs and outputs. There are several types of correlations that can be calculated: simple, rank, and partial. **Simple correlation** measures the strength and direction of a **linear** relationship between variables. Simple correlation refers to correlations performed on the actual input and output data, calculated by the **Pearson correlation coefficient**. For example, the Pearson correlation between input  $X$  and output  $Y$  is given by  $\rho(X, Y)$  [13]:

$$\rho_{(X,Y)} = \frac{\text{cov}(X, Y)}{\sqrt{\text{var}(X) \cdot \text{var}(Y)}} = \frac{E[(X - \bar{x})(Y - \bar{y})]}{\sigma_X \sigma_Y} \approx \frac{n \sum x_i y_i - \sum x_i \sum y_i}{\sqrt{n \sum x_i^2 - (\sum x_i)^2} \sqrt{n \sum y_i^2 - (\sum y_i)^2}} \quad (1)$$

The Pearson correlation is +1 in the case of a perfect positive (increasing) linear relationship, -1 in the case of a perfect decreasing (negative) linear relationship, and some value between -1 and 1 in all other cases. A simple correlation near zero means there is not a linearly organized relationship between the variables. Figure 2 shows some example correlation patterns and corresponding correlation coefficients. Note that if two variables are independent, they will have zero correlation but the converse is not true: they may have zero or near-zero correlation but show a strongly organized nonlinear relationship (e.g. see the last row of Figure 5). The best way to identify such zero-correlation but strongly patterned relationships is to plot them in a scatterplot as shown in Figure 2.



Source: <http://en.wikipedia.org/wiki/Correlation>

**Figure 2: Example Correlation Relationships**

**Rank correlations** refer to correlations performed on the ranks of the data. Ranks are obtained by replacing the actual data by the ranked values, which are obtained by ordering the data in ascending order. For example, the smallest value in a set of input samples would be given a rank 1, the next smallest value a rank 2, etc. Rank correlations are useful when some of the inputs and outputs differ greatly in magnitude; then it is easier to compare if the smallest ranked input sample is correlated with the smallest ranked output, for example. Rank correlations can also be used when monotonic nonlinear relationships exist. A rank correlation coefficient is also called a **Spearman correlation coefficient**. Partial correlation coefficients are similar to simple correlations, but a **partial correlation coefficient** between two variables measures their correlation while adjusting for the effects of the other variables. For the OECD case study, we used the Spearman correlation coefficient.

### 2.3 Sensitivity Analysis: Variance-based Decomposition

The correlation coefficients described in Section 2.2 only detect a linear or monotonic relationship. In contrast, the *variance-based indices* (also referred to as *Sobol' indices*) are not limited in this way. The **variance-based indices** identify the fraction of the variance in the output that can be attributed to an individual variable alone or with interaction effects [12,14]. There are two classes of variance-based sensitivity indices: *main effects* and *total effects*. The **main effects indices**,  $S_i$ , identify the fraction of uncertainty in the output  $Y$  attributed to input  $X_i$  alone. The **total effects indices**,  $T_i$ , correspond to the fraction of the uncertainty in output  $Y$  attributed to  $X_i$  and its interactions with other variables. These sensitivity indices are represented as:

$$S_i = \frac{\text{Var}(E(Y | X_i))}{\text{Var}(Y)} \quad (2)$$

$$T_i = \frac{E[\text{Var}(Y | X_{-i})]}{\text{Var}(Y)} \quad (3)$$

where  $\text{Var}(\cdot)$  is the variance,  $E(\cdot)$  is the expected value, and  $E(Y|X_i)$  is the expected value of  $Y$  conditioned on  $X_i$ .  $\text{Var}(Y|X_{-i})$  is the variance of  $Y$  conditioned on all the inputs except  $X_i$ . These indices involve multidimensional integrals that are evaluated approximately in practice. Note that each  $S_i$  varies between 0 and 1. Values close to 1 mean that the uncertainty in variable  $X_i$  is very significant in contributing to the uncertainty in output  $Y$ . The sum of  $S_i$  over all variables  $i$  must equal one. However, there are not the same restrictions on  $T_i$ . The values of  $T_i$  are greater than or equal to zero, but are not upper-bounded by one and their sum over all variables does not add to one.

The team led by Andrea Saltelli at the European Research Commission is generally credited with popularizing the use of variance-based indices for sensitivity analysis. In the past 10-15 years, several approaches have been developed for calculating the Sobol' sensitivity indices. The recent paper by [15] provides a detailed comparison of sampling approaches, with some comments about the relationship between the estimators and the sampling methods used.

Ideally, a full factorial sample would be performed with  $m$  samples taken in each of  $d$  input dimensions. Then, the integrals in the Sobol' formulas such as Equation 2 can easily be calculated given the  $m^d$  samples. However, a full factorial design may not be practical when each sample is an evaluation of a computationally costly function. Saltelli et al. [12] developed an approach which uses fewer samples,  $(2+d)m$  samples. Dakota uses a recent formulation [15] for the  $(2+d)m$  samples that has been improved to remove bias and better capture interaction effects. The actual formulas are described in [16]. Even with these formulas that reduce the number of function evaluations, often the only computational feasible approach to calculate the sensitivity indices is to employ a "surrogate" or emulator model in place of the expensive simulation model. A surrogate might be a neural network, a Gaussian process model, a spline, or a regression model. In this study, we used quadratic regression models in the calculation of the sensitivity indices.

### 3. OECD CASE 2A RESULTS

The case study of OECD Case 2a involved 17 input parameters with the distributions shown in Table 1. Note that most of the parameters were specified with normal distributions. The first four parameters (system pressure through inlet temperature) were core boundary condition parameters. The next six (cladding inner diameter through rod fill pressure) were listed in the category of manufacturing tolerance/geometric uncertainties. The final seven parameters were user-defined parameters, mainly focused on properties relating to the fuel, the cladding, and the gap.

Uncertain Parameter	Distribution		
	Type	Parameter 1	Parameter 2
System Pressure [Pa]	Normal	$1.551 \times 10^7$	51648.3
Mass Flux [ $\text{kg/m}^2\text{s}$ ]	Normal	3460.0	57.67
System Power [W/m]	Normal	1.0	0.016667
Inlet Temperature [K]	Uniform	558.0	564.0
Cladding ID [m]	This is a derived quantity: Cladding ID = Pellet OD + 2*gap_thickness		
Cladding Thickness [m]	Normal	$6.7 \times 10^{-4}$	$8.3 \times 10^{-6}$
Cladding Roughness [m]	Normal	$5.0 \times 10^{-7}$	$1.0 \times 10^{-7}$
Fuel Pellet Radius [m]	Normal	$4.7 \times 10^{-3}$	$3.335 \times 10^{-6}$
Fuel Density [ $\text{kg/m}^3$ ]	Normal	10299.24	51.4962
Fuel Pellet Roughness [m]	Normal	$2.0 \times 10^{-6}$	$1.6667 \times 10^{-7}$
Rod Fill Pressure [Pa]	Normal	$1.2 \times 10^6$	40000.0
Solid Fuel Swelling $\pm 20\%$ [-]	Normal	$5.58 \times 10^{-5}$	$5.577 \times 10^{-6}$
Clad Creep Rate $\pm 30\%$ [ $\text{s}^{-1}$ ]	Normal	1.0	0.15
Fuel Thermal Conductivity $\pm 10\%$ [W/m-K]	Normal	1.0	0.05
Clad Thermal Conductivity $\pm 5$ W/m-K	Normal	16.0	2.5
Fuel Thermal Expansion $\pm 15\%$	Normal	$1.0 \times 10^{-5}$	$7.5 \times 10^{-7}$
Gas Conductivity $\pm 5\%$ [W/m-K]	Normal	1.0	0.025
Gap Thickness [m]	Normal	$9.0 \times 10^{-5}$	$8.33 \times 10^{-6}$

**Table 1. Input Distributions used for Case 2a, OECD Fuels Benchmark study.**

The output responses included the centerline fuel temperature at 13 axial locations listed in Table 2:

Axial Node	Location (mm)
1 (bottom)	140.7
2	422
3	703.4
4	984.7
5	1266.1
6	1547.4
7	1828.8
8	2110.2
9	2391.5
10	2672.9
11	2954.2
12	3235.6
13 (top)	3516.9

**Table 2. Location of centerline temperatures reported for Case 2a, OECD Benchmark.**

In addition, there were 11 additional responses of interest listed in Table 3:

Maximum Fuel Centerline Temperature [K]
Maximum Cladding Surface Temperature [K]
Fission Gas Fraction[ % ]
Cladding Creep Strain [ - ]
Axial Elongation [ $\mu\text{m}$ ]
Fuel Thermal Expansion Coefficient [1/K]
Cladding Thermal Conductivity [W/m*K]
Cladding Thermal Exp Coefficient [K]
Fuel Radial Disp
Cladding Radial Disp
Gap Width [ $\mu\text{m}$ ]

**Table 3. Additional responses of interest, Case 2a, OECD Benchmark study.**

Note that all of these responses were requested at 8 burnup levels: 0, 5, 10, 20, 30, 40, 50, and 60 GWd/MTU, respectively. This made for a very large number of quantities to track and record. Although Dakota helped automate this process significantly, there still was some manual manipulation involved to get the final sensitivity and uncertainty analysis number into the spreadsheet that OECD provided.

As mentioned above, we ran 300 BISON samples, using a LHS sampling study generated in Dakota. The Dakota input deck for this study is provided in Appendix A. The results were compiled in a spreadsheet provided by OECD to allow for consistent comparison of results across various groups and codes. This spreadsheet is available by contacting the authors of this report. Additionally, Kyle Gamble presented a summary of the results at the OECD UAM working group meeting in May, 2015 in Spain. Kyle's presentation is also available upon request. Below, we present some summary figures from the Case 2a study which represents the types of output analysis that can be performed.



Figures 3 and 4 contain scatterplots of centerline temperature at 3 locations vs. user-defined uncertainties at burnup levels of 5 and 50 GWd/MTU, respectively. As mentioned, scatterplots provide a visual representation of sensitivity analysis results. Specifically, one can see that the fuel thermal conductivity is strongly negatively correlated with temperatures at the 3 locations for both burnup levels. As the thermal conductivity of the fuel increases, the temperatures decrease. Further, one can see that the relationship is even tighter (e.g. a more negative correlation coefficient) at a burnup of 50 GWd/MTU than at a burnup of 5. The Spearman correlation coefficients between the fuel thermal conductivity at locations 1, 7, and 13 are -0.64, -0.70, and -0.65 for burnup of 5 GWd/MTU while they are -0.88, -0.90, and -0.88 for a burnup of 50 GWd/MTU, respectively. Similarly, one can see that the gap thickness is positively correlated with the temperature values at a burnup of 5 GWd/MTU but has little correlation at a burnup of 50 GWd/MTU because the gap has closed at that burnup level.

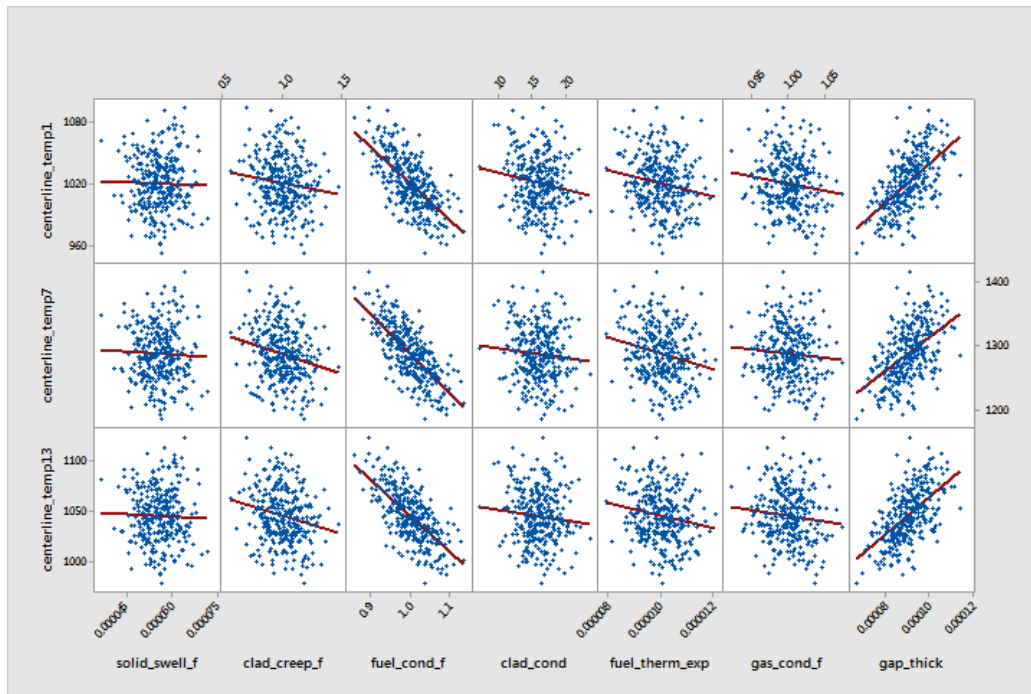


**Figure 3: Scatterplots of Centerline temperature at 3 locations vs. User-defined Uncertainties, Burnup = 5 GWd/MTU**

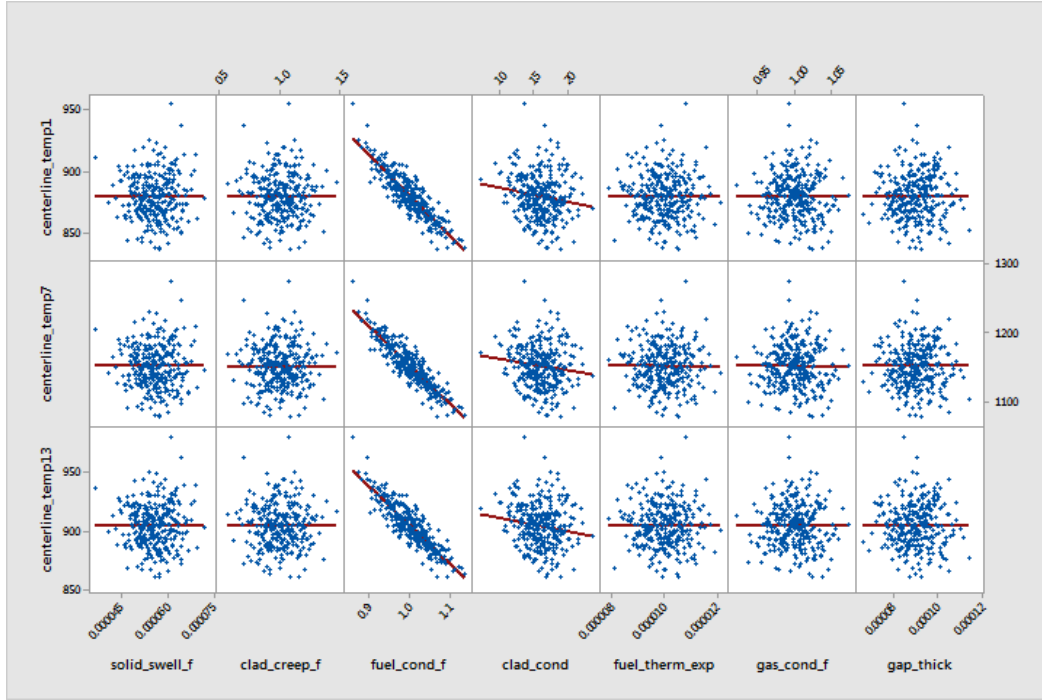


**Figure 4: Scatterplots of Centerline temperature at 3 locations vs. User-defined Uncertainties, Burnup = 50 GWd/MTU**

Figures 5 and 6 show scatterplots of the percentage fission gas released (FGR) as a function of the user-defined uncertainties at burnup levels of 5 and 50 GWd/MTU, respectively. Note that the vertical axis scales are different: most of the 300 samples have a FGR percentage of less than 0.01% at 5 GWd/MTU, but the FGR at 50 GWd/MTU is around 1% with a few samples up near 2%. Again, thermal conductivity of the fuel has a strong influence on the FGR.

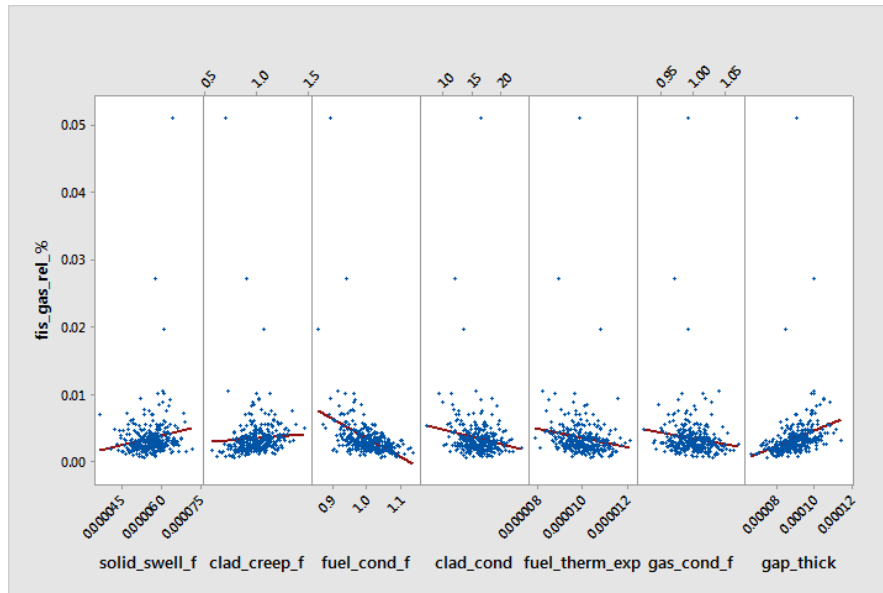


**Figure 5: Scatterplots of Fission Gas Release Percentage vs. User-defined Uncertainties, Burnup = 5 GWd/MTU**

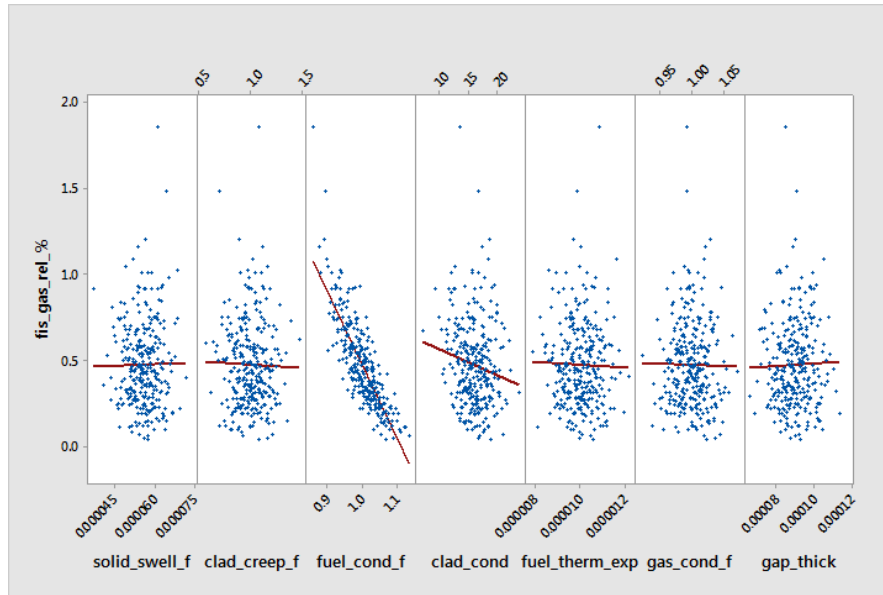


**Figure 6: Scatterplots of Fission Gas Release Percentage vs. User-defined Uncertainties, Burnup = 50 GWd/MTU**

Figure 7 shows an example histogram of the 300 samples for centerline temperature at location 7. This gives an indication of the uncertainty in the results based on the uncertainty in the input distributions shown in Table 1. At location 7 at a burnup of 50GWd/MTU, the centerline temperature varies from a minimum of 1077K to a max of 1274K, with a mean of 1152K. This particular response is well approximated by a normal distribution, as shown by the red PDF in Figure 7.

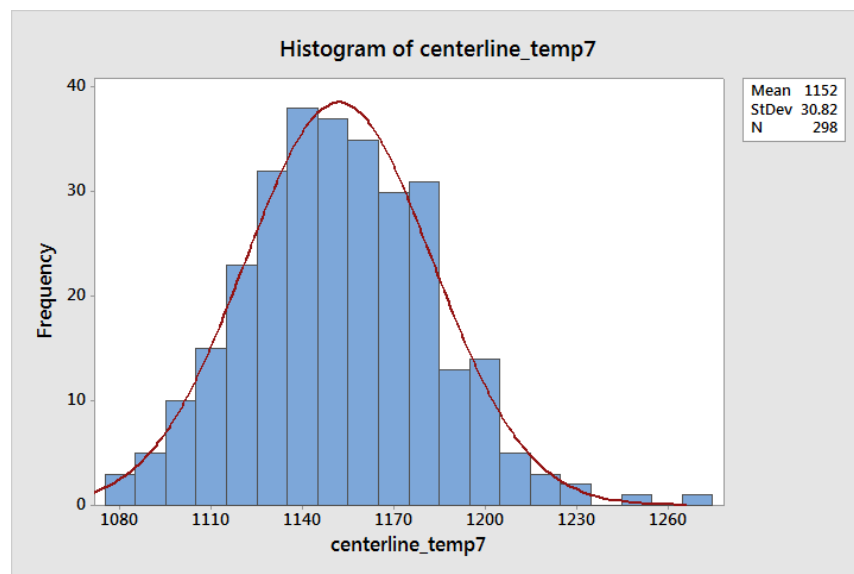


**Figure 7: Histogram of 300 samples of Centerline temperature at location 7 (degrees K), for a Burnup = 50 GWd/MTU**

Correlation tables were produced for all of the inputs and outputs. Figure 8 shows one example, where the inputs are given by the rows, and the some of the outputs are shown in the columns. The correlations are highlighted so that red indicates very strong correlations with absolute value greater than 0.6, and yellow shows medium correlations between 0.3 and 0.6. Figure 8 indicates that the thermal conductivity of the fuel is strongly negatively correlated with the maximum fuel centerline temperature (first column, correlation coefficient = -0.885), and also negative correlated with the FGR percentage. The clad creep is strongly positively correlated with cladding creep strain (second last column, correlation coefficient of 0.986) and negatively correlated with axial elongation. Inlet temperature is strongly positively correlated with maximum cladding surface temperature (second column, correlation coefficient of 0.893). These types of correlation tables can be very useful for identifying parameters that strongly affect output behavior of various responses.

Burnup (GWd/MTU):	Output Parameter:	Maximum Fuel Centerline Temperature [K]		Maximum Cladding Surface Temperature [K]		Fission Gas Fraction [%]		Cladding Creep Strain [-]		Axial Elongation [μm]	
		Nominal	st dev.	Nominal	st dev.	Nominal	st dev.	Nominal	st dev.	Nominal	st dev.
		1152.0738	30.8162	594.8518	1.7663	0.4747	0.2532	0.0142	0.0020	7062.6090	4609.5143
50	Uncertainty Parameter:	Spearman's RCC		Spearman's RCC		Spearman's RCC		Spearman's RCC		Spearman's RCC	
	System Pressure	-0.022		-0.032		-0.018		0.040		-0.033	
	Mass Flux	-0.033		-0.238		-0.036		-0.038		0.036	
	Linear Power	0.342		0.275		0.432		-0.039		-0.030	
	Inlet Temperature	0.038		0.893		0.040		0.052		-0.044	
	Cladding ID										
	Cladding Thickness	0.039		0.041		0.038		-0.076		0.073	
	Cladding Roughness	0.035		0.034		0.039		0.010		0.005	
	Fuel Pellet OD	0.008		0.010		-0.003		0.054		-0.042	
	Fuel Density	-0.181		-0.035		-0.193		0.044		0.001	
	Fuel Pellet Roughness	0.050		0.002		0.051		0.008		-0.020	
	Rod Fill Pressure	-0.020		-0.004		-0.014		-0.060		0.041	
	Solid Swelling [-]	-0.012		-0.004		-0.012		-0.034		-0.250	
	Clad Creep [s]	-0.018		0.043		-0.033		0.986		-0.823	
	Fuel Conductivity [W/m-K]	-0.885		0.002		-0.831		0.057		0.024	
	Clad Conductivity [W/m-K]	-0.119		-0.049		-0.139		0.002		0.128	
	Fuel Therm Exp [1/K]	-0.020		-0.024		-0.033		-0.027		-0.099	
	Gas Conductivity [W/m-K]	-0.022		0.026		-0.024		0.021		-0.019	

**Figure 8: Correlation Table of various input/output correlations for a Burnup = 50 GWd/MTU**

Finally, we also performed the Sobol' variance-based decomposition to obtain sensitivity indices as described in Section 2.3. This required the use of surrogate models to approximate the responses, since this method requires thousands of function evaluations to calculate the sensitivity indices. We performed this analysis using the Dakota input deck shown in Appendix B. This particular study took 5000\*(2+17)=95000 evaluations to perform. We used the original 300 BISON runs to perform this study. Dakota constructed quadratic polynomial surrogate models for each response based on the BISON runs as training data. The 95000 evaluations were then performed on the surrogate model. The quadratic polynomial surrogates were of the form:

$$\hat{y}(x) = \sum_{i=1}^d a_i x_i + \sum_{i=1}^d b_i x_i^2 + \sum_{i=1}^d \sum_{k=i+1}^d c_{ik} x_i x_k$$

where  $\hat{y}$  is the response predicted by the surrogate,  $x$  is the d-dimensional input variable (in our case, d=17), and the coefficients of the polynomial terms are  $a_i$ ,  $b_i$ , and  $c_{ik}$ . For the 17-d problem, we had 171 basis terms in the surrogate model given above. Most of the responses were well-approximated with this surrogate, with R-squared values generally near 1.0.

Figure 9 shows a table of results for the centerline temperature at location 7 and for the FGR percentage. The first two columns indicate that the main and total effects are about the same for this centerline temperature, indicating that there are not strong interaction effects between variables. The main effects index for the fuel thermal conductivity (fuel\_cond\_f) indicates that 70% of the variance in centerline temperature at location 7 can be explained by the variance in the fuel thermal conductivity. The system power factor contributes to 10% of the variance, with the remaining variables contributing small amounts. The main effects column sums to 1.0 for the centerline\_temp7, indicating that the variance of this response is well explained by the variance of the individual parameters. The conclusions are different for the FGR percentage. The fuel thermal conductivity only contributes to about 20% of the variance, and the sum of the main effects column is only about .45, meaning that 45% of the variance is explained by main effects. The total effects column has some values that are quite different from the main effects, indicating that there are significant interactions between variables that contribute to the overall variance of the FGR percentage. For example, the system power factor has a main effect index of only 0.063 but a total effect index of 0.21, and the fuel thermal conductivity total effects index increases from 0.21 to 0.42. Further statistical analysis would be required to quantify which combinations of variables (e.g. pairwise terms) most influence the overall variance of the FGR percentage.

Input Variable	Sobol' Indices			
	centerline_temp7		fis_gas_rel_%	
	Main	Total	Main	Total
sys_pressure	7.9E-05	1.1E-04	1.5E-02	6.1E-02
cool_flow_rate	2.7E-05	5.0E-05	3.6E-04	3.1E-02
sys_pow_fac	1.0E-01	1.0E-01	6.3E-02	2.1E-01
clad_thick	1.0E-03	8.5E-04	4.7E-03	3.7E-02
clad_rough	1.2E-03	9.6E-04	1.5E-02	7.7E-02
fp_out_rad	2.2E-04	9.5E-05	7.4E-03	7.8E-02
fuel_density	4.8E-02	4.3E-02	6.2E-03	8.5E-02
fuel_rough	2.1E-03	2.7E-03	2.0E-02	4.8E-02
fill_pressure	5.6E-04	1.7E-04	2.1E-03	3.8E-02
solid_swell_f	3.9E-03	2.6E-03	1.9E-03	7.5E-02
clad_creep_f	6.3E-02	6.3E-02	1.6E-02	1.0E-01
fuel_cond_f	7.0E-01	7.1E-01	2.1E-01	4.2E-01
clad_cond	9.7E-03	1.0E-02	1.8E-02	6.4E-02
fuel_therm_exp	5.5E-02	5.9E-02	9.8E-03	9.0E-02
gas_cond_f	6.9E-03	6.9E-03	5.2E-02	1.2E-01
gap_thick	4.7E-03	7.8E-03	7.1E-04	3.2E-03
in_fluid_temp	-3.9E-05	2.4E-04	1.0E-02	7.0E-02

**Figure 9: Sobol' indices for Centerline temperature at location 7 and for percentage of Fission Gas released, for a Burnup = 50 GWd/MTU**



## **4. CONCLUSIONS**

In this report, we present a sensitivity analysis and uncertainty quantification study for Case 2a of the Fuels Benchmark problems defined by the OECD Uncertainty Analysis in Modeling working group. We discussed the BISON and Dakota software used, provided information about the sensitivity and uncertainty analysis methods, and presented some results. We plan on performing further case studies and participating in the benchmark exercises as time and funding permits.

## 5. REFERENCES

1. Blyth, T., N. Porter, M. Avramova, K. Ivanov, E. Royer, E. Sartori, O. Cabellos, H. Feroukhi, E. Ivanov. "Benchmark for Uncertainty Analysis in Modelling (UAM) for Design, Operation, and Safety Analysis of LWRs. Volume II: Specification and Support Data for the Core Cases (Phase II). Nuclear Energy Agency/Nuclear Science Committee of the Organization for Economic Cooperation and Development. NEA/NSC/DOC (2014), Version 2.0.
2. Williamson, R.L., J.D. Hales, S.R. Novascone, M.R. Tonks, D.R. Gaston, C.J. Permann, D. Andrs and R.C. Martineau, "Multidimensional multiphysics simulation of nuclear fuel behavior," *J. Nucl. Materials*, **423**, pp. 149-163, 2012. Available at: <http://dx.doi.org/10.1016/j.jnucmat.2012.01.012>.
3. Gaston, D., C. Newman, G. Hansen and D. Lebrun-Grandi, "MOOSE: A parallel computational framework for coupled systems of nonlinear equations," *Nucl. Eng. Design*, **239**, pp. 1768-1778, 2009. Available at <http://dx.doi.org/10.1016/j.nucengdes.2009.05.021>.
4. Perez, D.M., R. L. Williamson, S. R. Novascone, T. K. Larson, J. D. Hales, B.W. Spencer, and G. Pastore, "An Evaluation of the Nuclear Fuel Performance Code BISON." *International Conference on Mathematics and Computational Methods Applied to Nuclear Science and Engineering*, 2013.
5. Hales, J.D., R. L. Williamson, S. R. Novascone, G. Pastore, B. W. Spencer, D. S. Stafford, K. A. Gamble, D. M. Perez, and W. Liu. *BISON Theory Manual: The Equations Behind Nuclear Fuel Analysis*. Technical Report INL/EXT-13-29930, Rev.1, Idaho National Laboratory, September 2014.
6. Adams, B.M., Bohnhoff, W.J., Dalbey, K.R., Eddy, J.P., Eldred, M.S., Gay, D.M., Haskell, K., Hough, P.D., and Swiler, L.P., "*DAKOTA, A Multilevel Parallel Object-Oriented Framework for Design Optimization, Parameter Estimation, Uncertainty Quantification, and Sensitivity Analysis: Version 5.0 User's Manual*," Sandia Technical Report SAND2010-2183, December 2009. Updated December 2010 (Version 5.1), November 2011 (Version 5.2), February 2013 (Version 5.3), and May 2013 (Version 5.3.1).
7. Swiler, L. P. and G. D. Wyss. "A User's Guide to Sandia's Latin Hypercube Sampling Software: LHS Unix Library/Standalone Version." Technical Report SAND2004-2439. Sandia National Laboratories, Albuquerque NM.
8. Iman R.L. and W.J. Conover. Small Sample Sensitivity Analysis Techniques for Computer Models, with an Application to Risk Assessment. *Communications in Statistics: Theory and Methods* 1980;A9(17):1749-1842.
9. Owen, A. B. (1992). A central limit theorem for Latin hypercube sampling, *Journal of the Royal Statistical Society Series B* 54, 13, pp. 541–551.
10. Stein. M. Large sample properties of simulations using Latin hypercube sampling. *Technometrics*, 29(2):143–51, 1987.
11. Saltelli, A., Chan, K., Scott, E.M. *Sensitivity Analysis*. New York: Wiley; 2000.
12. Saltelli, A., Tarantola, S., Campolongo, F., Ratto, M. *Sensitivity Analysis in Practice: A Guide to Assessing Scientific Models*. New York: Wiley; 2004.
13. Larsen, R. J. and M. L. Marx. *An Introduction to Mathematical Statistics and its Applications*, 2<sup>nd</sup> ed. Prentice-Hall. Edgewood Cliffs, NJ: 1986.



14. Sobol', I.M. *Sensitivity analysis for non-linear mathematical models*. Mathematical Modeling and Computational Experiment 1993;1:407–414.
15. Saltelli, A., Annoni, P., Azzini, I., Campolongo, F., Ratto, M., Tarantola, S. “Variance based sensitivity analysis of model output. Design and estimator for the total sensitivity index.” Computer Physics Communication 2010;181:259 – 270.
16. Weirs, V.G., Kamm, J. R., Swiler, L.P., Ratto, M., Tarantola, S., Adams, B.M., Rider, W.J. and Eldred, M.S., “Sensitivity Analysis Techniques Applied to a System of Hyperbolic Conservation Laws.” 107, *Reliability Engineering and System Safety*, November 2012, pp.157-170. doi:10.1016/j.ress.2011.12.008.
17. Ross, A.M. and Stoute, R.L. “Heat Transfer Coefficient between UO<sub>2</sub> and Zircaloy-2”. AECL-1552, 1962.

## APPENDIX A

Dakota input file to generate 300 LHS samples of a BISON model varying 17 parameters, and extracting 24 responses:

```
# DAKOTA INPUT FILE

environment,
    tabular_graphics_data

method,
    sampling
    sample_type lhs
    samples = 300
    seed = 3487

variables,
    normal_uncertain = 16
    means = 1.55E+07 3460. 1. 6.70E-04 5.00E-07 4.70E-03 10299.24
2.00E-06 1.20E+06 5.58E-05 1. 1. 16. 1.00E-05 1. 9.0E-5
    std_deviations = 51648.3 57.67 0.016667 0.00000833 0.0000001
0.000003335 51.4962 1.66667E-07 40000.0 0.000005577 0.15 0.05 2.5
0.00000075 0.025 8.33E-6
    descriptor 'sys_pressure' 'cool_flow_rate' 'sys_pow_fac'
'clad_thick' 'clad_rough' 'fp_out_rad' 'fuel_density' 'fuel_rough'
'fill_pressure' 'solid_swell_f' 'clad_creep_f' 'fuel_cond_f' 'clad_cond'
'fuel_therm_exp' 'gas_cond_f' 'gap_thick'
    uniform_uncertain = 1
    lower_bounds = 558
    upper_bounds = 564
    descriptors = 'in_fluid_temp'

interface,
    system
    analysis_driver = 'run_submission'
    parameters_file = 'params.in'
    results_file = 'results.out'
    file_save file_tag aprepro

responses,
    num_response_functions = 24
    descriptors = 'average_burnup' 'centerline_temp1' 'centerline_temp2'
'centerline_temp3' 'centerline_temp4' 'centerline_temp5' 'centerline_temp6'
'centerline_temp7' 'centerline_temp8' 'centerline_temp9' 'centerline_temp10'
'centerline_temp11' 'centerline_temp12' 'centerline_temp13'
'max_centerline_temp' 'max_clad_surf_temp' 'max_clad_creep_strain'
'clad_elongation' 'fis_gas_generated' 'fis_gas_released' 'fuel_radial_disp'
'clad_radial_disp' 'gap_thick' 'avg_therm_cond_fuel'
    no_gradients
    no_hessians
```

## APPENDIX B

Dakota input file to generate Variance-based sensitivity indices, using a quadratic polynomial surrogate model for each response. The surrogates are constructed over 300 LHS samples of a BISON model with 17 parameters and 24 responses. The LHS results are in the file “dakota\_tabular5.dat”, the results at a burnup of 5 GWd/MTU.

```
environment
    tabular_graphics_data
    method_pointer = 'UQ'

method,
    id_method = 'UQ'
    model_pointer = 'SURR'
    output verbose
    sampling
    sample_type lhs
    samples = 5000
    seed = 5034
    variance_based_decomp

model,
    id_model = 'SURR'
    surrogate global,
    import_points_file = 'dakota_tabular5.dat' custom_annotated
header eval_id
    polynomial quadratic
    #neural_network
    #mars
    #gaussian_process surfpack

variables,
    normal_uncertain = 16
    means = 1.55E+07 3460. 1. 6.70E-04 5.00E-07 4.70E-03 10299.24
2.00E-06 1.20E+06 5.58E-05 1. 1. 16. 1.00E-05 1. 9.0E-5
    std_deviations = 51648.3 57.67 0.016667 0.00000833 0.0000001
0.000003335 51.4962 1.66667E-07 23333.33333 0.000005577 0.15 0.05
2.5 0.00000075 0.025 0.125E-5
    descriptor 'sys_pressure' 'cool_flow_rate' 'sys_pow_fac'
'clad_thick' 'clad_rough' 'fp_out_rad' 'fuel_density' 'fuel_rough'
'fill_pressure' 'solid.swell_f' 'clad_creep_f' 'fuel_cond_f' 'clad_cond'
'fuel_therm_exp' 'gas_cond_f' 'gap_thick'
    uniform_uncertain = 1
    lower_bounds = 558
    upper_bounds = 564
    descriptors = 'in_fluid_temp'

interface,
    id_interface = 'I1'
    direct
    analysis_driver = 'text_book'

responses,
    num_response_functions = 24
```

```
        descriptors = 'average_burnup' 'centerline_temp1'  
'centerline_temp2' 'centerline_temp3' 'centerline_temp4'  
'centerline_temp5' 'centerline_temp6' 'centerline_temp7'  
'centerline_temp8' 'centerline_temp9' 'centerline_temp10'  
'centerline_temp11' 'centerline_temp12' 'centerline_temp13'  
'max_centerline_temp' 'max_clad_surf_temp' 'max_clad_creep_strain'  
'clad_elongation' 'fis_gas_generated' 'fis_gas_rel_%' 'fuel_radial_disp'  
'clad_radial_disp' 'gap_thick' 'avg_therm_cond_fuel'  
        no_gradients  
        no_hessians
```

## DISTRIBUTION

1 Marius Stan  
National Technical Directory NEAMS  
Argonne National Laboratory  
9700 S. Cass Avenue  
Argonne, IL 60439

1 Dave Pointer  
National Technical Directory NEAMS  
Argonne National Laboratory  
9700 S. Cass Avenue  
Argonne, IL 60439

1 Jason Hales  
Idaho National Laboratory  
2525 Fremont Avenue  
Idaho Falls, ID 83415

1 Richard Williamson  
Idaho National Laboratory  
2525 Fremont Avenue  
Idaho Falls, ID 83415

1	MS 0748	R.O. Gauntt	06232
1	MS 1318	J.R. Stewart	01441
1	MS 1318	B.M. Adams	01441
1	MS 1318	V.A. Mousseau	01444
1	MS 0899	RIM - Reports Management, 9532 (electronic copy)	

